AIChE WILEY InterScience DISCOVER SOMETHING GREAT

FLUID MECHANICS AND TRANSPORT PHENOMENA

Enhancing Flow Boiling and Antifouling with Nanometer Titanium Dioxide Coating Surfaces

Ming-Yan Liu
School of Chemical Engineering and Technology, Tianjin University, Tianjin 300072, China;
State Key Laboratory of Chemical Engineering (Tianjin University), Tianjin 300072, China

Hong Wang and Yan Wang
School of Chemical Engineering and Technology, Tianjin University, Tianjin 300072, China

DOI 10.1002/aic.11150
Published online March 15, 2007 in Wiley InterScience (www.interscience.wiley.com).

This article aims to develop a new heat-transfer surface on which both heat-transfer enhancement and fouling prevention can be observed. One of the potential methods is to coat a thin layer on the heat-transfer surface with nanometer material. The selection of coated nanometer material, the preparation, and characterization of nanometer coatings on heat-transfer surface, including the measurement and calculation of the coated thickness, contact angle and surface free energy, the experiments on heat transfer of flow boiling and antifouling are all investigated in this article. The results declare that heat-transfer film coefficients of flow boiling on TiO_2 coating surfaces with film thickness of 1.41×10^{-7} and 1.587×10^{-6} m are higher than those on uncoated surface of heated tube. The fouling resistance on the surface modified with nanometer material is lower than that on the untreated heat-transfer surface and remains constant during a long operating time. Under present experimental conditions, the coated heat-transfer surface with thin film thickness of 1.41×10^{-7} m is the best one in enhancing heat transfer of flow boiling and preventing fouling, since its surface free energy is the lowest one.
 AIChE J, 53: 1075–1085, 2007
Keywords: surface coatings, enhancing heat transfer, antifouling, thin film, nanometer, coated layer, titanium dioxide

Introduction

Since the middle of the 20th century, the flow boiling equipments have extensively been applied in a series of process industries. However, there are some troublesome problems such as the fouling on heat-transfer surface and boiling heat-transfer deterioration, etc. Hence, a lot of research on these problems were carried out, and some achievements were made. For example, the enhancing methods on boiling heat transfer[1–4] as well as the ways of antifouling or scale cleaning[1,5,6] were developed and reviewed. Among proposed or applied techniques, surface treatment or surface modification technique to reduce the surface free energy was paid great attention recently.

Mueller-Steinhagen et al.[7] made attempts to reduce the stickiness of the deposit fouling by coating the heat-transfer surface with Teflon and the experiments were performed with New Zealand Forest Products Kraft black liquor to measure heat-transfer coefficients and fouling rates during convective and subcooled flow boiling heat transfer. It was found that the operation time until severe fouling occurred was significantly prolonged. However, after about 18,000 s, the Teflon coating exhausted.

Correspondence concerning this article should be addressed to M.-Y. Liu at myliu@tju.edu.cn.

Muller-Steinhagen et al.[8] developed a stainless steel surface with low surface free energy by ion implantation. Fouling experiment during pool boiling of $CaSO_4$ solution demonstrated that fouling was significantly reduced for all of the heat flux and $CaSO_4$ concentration. Ren et al.[9] obtained similar results.

Muller-Steinhagen et al.[10] investigated the effects of surface free energy and surface roughness on the deposition of $CaSO_4$ during convective and subcooled flow boiling heat-transfer to aqueous $CaSO_4$ solutions. The surfaces of several test heaters were treated by ion beam implantation, unbalanced magnetron sputtering, mixed sputtering, and plasma arc deposition to reduce surface free energy. One heater was electropolished to reduce surface roughness and one was etched by an electrochemical method to increase surface roughness. Fouling runs with these heaters, and with an untreated surface as control, were carried out at different heat fluxes, flow velocities, and salt concentrations. Heat-transfer surfaces with low surface free energy experienced significantly reduced fouling.

Recently, the surface modification technique is applied to solve the fouling problem in dairy industry.[11,12] Santos et al.[11] applied ion implantation, diamond-like carbon sputtering, plasma enhanced chemical vapor deposition, and autocatalysis methods to treat the stainless steel surfaces and to characterize them according to the chemical composition, roughness, topography, and wettability. X-ray photoelectron spectroscopy and X-ray microanalysis were applied to determine the surface chemical composition. Atomic force microscopy and stylus-type instruments were used for roughness determination, and the surface topography was imaged with atomic force microscopy and scanning electron microscopy. The contact angle and surface tension were measured with the Wilhelmy plate method and the sessile drop method. For thick modified layers only the elements of the coating were detected at the surface, whereas for thin layers the surface composition determined was that of the stainless steel substrate. Rosmaninho and Melo[12] studied the relationship between calcium phosphate fouling behavior and the treated surface properties. The results indicated that fouling caused by calcium phosphate is affected by the surface free energy properties of the metal substrata since different surfaces develop different deposit structures.

In spite of the many studies devoted to finding ways to avoid fouling or to enhance boiling heat transfer, no major break-through has been reported that can provide the process industries with both preventing fouling on boiling surface and enhancing heat transfer. However, recent developments in surface treatment technology and nanometer technology have opened up new possibilities.

The researches and applications of nanometer technology on heat-transfer process are mainly focused on the nanometer fluids as a high efficient heat transfer medium[13,14] and little work is concerned on the surface modification with nanometer materials to enhance boiling heat transfer[15–19] and to prevent fouling.

It is well known that titanium dioxide, TiO_2, is a photocatalyst with a unique characteristic and the affinity for water can be changed when exposed to UV light. This nature gives a self-cleaning effect to the coated surface and has already been applied to some construction materials, car coatings and so on. Clearly, it is very interesting to explore its potential application in boiling heat-transfer process.

Takata et al.[15–18] applied the superhydrophilicity to enhance heat transfer of pool boiling, immersion cooling, falling film evaporation, and single water drop evaporation on treated metal surfaces by dipping, sputtering or plasma-irradiating process with film thickness of micrometer order. The main results are as following. A TiO_2-coated specimen cooled down more rapidly than a noncoated one because the film boiling regime breaks down at higher temperature and the minimum heat flux (MHF) point shifted to higher temperature by the increase in surface wettability. The heat-transfer coefficient of falling film evaporation of TiO_2-coated surface was about 40 times higher than that of noncoated surface because a thin stable film can be realized even in a low flow rate region. The critical heat flux (CHF) of TiO_2-coated surface is about two times larger than that of noncoated one.

Very recently, Takata et al.[19] reported their work on applying the superhydrophilic nature for the enhancement of pool boiling of water and evaporation of single water droplet and the main interest of the pool boiling experiment was focused on the effect of wettability on the CHF point and the experiment of droplet evaporation aimed to make clear the effect of contact angle on the evaporation time. The treated surfaces of copper and glass plate for pool boiling were coated by dipping process with a TiO_2 film thickness of 1×10^{-6} m and a sputtering method with a TiO_2 layer of 2.50×10^{-7} m in thickness. Heat-transfer surfaces for drop evaporator were coated by two different sputtering conditions; one was the surface sputtered by TiO_2 only, and the other was the surface that SiO_2-sputtered layer of $(1-20) \times 10^{-9}$ m was added on the TiO_2 layer. The main results were summarized as follows: (1) The TiO_2-sputtered surface exhibits excellent heat-transfer characteristics in nucleate boiling region and its CHF is higher than the noncoated surface. The MHF temperature is 100 K higher than that of noncoated surface. (2) Evaporation time decreases with the decrease in contact angle. (3) The experiments by concave surface depict that the wetting limit and the Leidenfrost temperatures, increase with the decrease in contact angle. The superhydrophilic surface can be an ideal heat-transfer surface and will be applicable to various heat-transfer phenomena that are affected by surface wettability.

The above work is an excellent beginning to explore the nanometer surface modification on enhancing phase change heat transfer. In this work, the heat-transfer enhancement of flow boiling and antifouling experimental investigations were conducted on the heat-transfer surfaces coated with nanometer TiO_2 thin layer with different film thickness made by liquid phase deposition (LPD) method. The experiments were carried out in a double-pipe heat exchanger with vapor–liquid external natural circulation flow boiling. The antifouling and enhancing heat-transfer mechanisms of the modified surface and the major influence factors were discussed.

Experimental

The first step of the whole experiment was to treat inner surface of the heat-transfer tube with the thin layer of nano-

meter material, TiO_2. The second one was to characterize the thin film, including measuring and calculating the thickness, contact angle and surface free energy of the thin layer. The last one was to carry out the experiments of flow boiling heat transfer and antifouling.

Preparation of heat-transfer tube with nanometer-coated layer

In this work, nanometer material TiO_2 was selected as the initial coating material of thin film due to its self-cleaning function resulted from the nanometer effects. The function has been tested for application in self-cleaning building window glass, car glass, and neck tie. The thin layer of TiO_2 was deposited on the inside surface of the inner tube in the double-pipe heat exchanger by LPD method.

The term "LPD" refers to the formation of oxide thin films from an aqueous solution of a metal-fluoro complex $[MFn]^{m-n}$ which is slowly hydrolyzed by adding water, boric acid (H_3BO_3), or aluminum metal. While the addition of water directly forces the precipitation of the oxide, boric acid and aluminum act as fluoride scavengers, which destabilize the fluoro complex and forces the oxide precipitation. It was first reported in the patent literature in 1980s and has been used for films, such as titania, silica, vanadia, tin oxide, iron oxyhydroxide, zirconia, etc., and has been widely tested for application in integrated circuit processing, and in metal-oxide-semiconductor and complementary metal-oxide-semiconductor technology etc. The principle of LPD is well known and it isn't necessary to give the explanation here and the further detail could be referred to the literature.[20,21]

The test samples for LPD method are seamless steel tubes. Prior to preparation of test samples, the tubes were cleaned by dilution solution of hydrogen nitrate, distilled water, dilution solution of sodium hydroxide and absolute ethyl alcohol to remove the grease, dust and rust and then were dried in drying oven at temperature of about 393.15 K. When the surface became dry, the samples were dipped into the homogeneous deposition solution in a deposition vessel under proper reaction conditions, including the ingredient concentrations, temperature, and time. After the reaction process, the test samples were heat treated, cleaned, and dried.

Characterization of heat-transfer tube with nanometer-coated layer

Measurement of Thin Layer Thickness. The analysis of film thickness can be performed in two different ways: (1) from the surface of a thin film or (2) from the cross-section of the film and there are several film thickness determining methods, such as prefabricated step analysis, composition analysis, weighing analysis, cross-sectional analysis etc. All these techniques have their own limitations. In this article, X-ray diffraction (XRD) method was applied to determine the thin film thickness. XRD is a rapid, nondestructive test that can provide information about the individual layer thickness, the composition modulation, and the interfacial roughness, as well as grain sizes and defect densities within the layer.[22–24] XRD can be roughly separated into two categories: small angle ($2\theta \leq 15^\circ$) and large-angle ($2\theta \geq 15^\circ$) XRD, and the large-angle was applied in this work. The XRD measurement was preformed with X-ray diffractiometer (Rigaku D/MAX 2200V/PC type) in the Analysis Center of Tianjin University. The film thickness was calculated according to the equation of diffraction intensity:

$$I = I_\infty \exp\left(\frac{-2\mu\delta}{\sin\theta}\right) \tag{1}$$

where I–XRD integrated intensity, counts·(s^{-1}), can be found from XRD plot;

I_∞ – XRD integrated intensity of bulk body, counts·(s^{-1}), can be found from XRD plot;

θ – diffraction angle (°), can be found from XRD plot;

μ – absorption coefficient, it is a constant, $\mu = 5491.1$;

δ – thickness of coated layer (m).

The three samples were intercepted from three prepared coated tubes, and are named sample A (uncoated surface), sample B (coated surface with thinner layer), and sample C (coated surface with thicker layer), respectively.

Figure 1 shows the XRD plots of the three samples. For the spikes in each sub-plot in Figure 1, the spike with the highest XRD integrated intensity indicates the existence of the substrate material iron (Fe). Table 1 lists the concerned values of diffraction intensity at given diffraction angle. For the diffraction intensity of the substrate Fe on the three samples, it is the largest on sample A (756 counts·s^{-1} at 44.28° in double diffraction angle), and the intensity deduces on the coated samples due to the existence of the coated thin layers (690 counts·s^{-1} at 44.22° for sample B and 597 counts·s^{-1} at

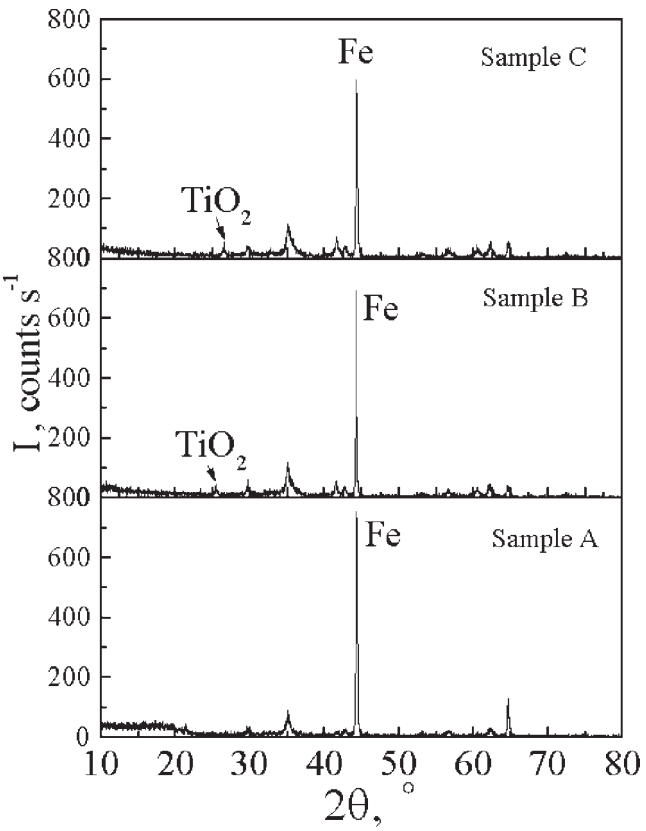

Figure 1. XRD patterns of the three samples of heat-transfer tubes.

Table 1. Values of Diffraction Intensity with Double Diffraction Angle

Sample	2θ (°)	I (Counts·s^{-1})
A	25.44	10
	44.28	756
B	25.44	45
	44.22	690
C	26.48	55
	44.28	597

44.28° for sample C). On the other hand, no spike is found on the XRD plot of sample A when double diffraction angle is about 25°. However, the spike at about 25° of 2θ is observed on the XRD curves of both sample B and sample C, as shown in Figure 1. These spikes represent the diffraction intensity of TiO_2 thin layer, and the intensity is different for different coated layer thickness. The higher the spike height or the intensity is, the thicker the film thickness is. Table 1 illuminates that the diffraction intensity varies from 10 to 55 counts·s^{-1} at about 25° in double diffraction angle and the double diffraction angle increases from 25.44 to 26.48°. Hence, the value and its variation of diffraction intensity of the substrate and coated layer can be used to judge the surface being coated or not and the film thickness being thick or thin.

The thickness values of the film for coated surfaces (samples B and C) are calculated by Eq. (1) and are listed in Table 2.

The surface appearance of the samples was observed by scanning electron microscope (Philips, XL-30 type SEM) as illustrated in Figure 2. The quality of SEM images is low due to the measuring equipments. However, one can generally see that in the TiO_2 thin film prepared by LPD method, the distribution of TiO_2 grain is even, and the structure of TiO_2 thin film is close. There is no needle cavity in it.

It is noted that according to the measuring principle of XRD method, the film thickness obtained represents the thickness of the whole sample surface, at least denoting the thickness of a line across the sample surface because the X-ray scans at least a line across the sample surface, not one point or one position. The thickness of the coating is considered to be uniform for the samples of the heated tube, and thus for the whole heat-transfer tube.

Measurement of Contact Angle. The contact angle (or wetting angle) is an important parameter in determining the surface tension or surface free energy for appearance of fouling layer. There are two methods to measure contact angle: direct measurement and weight measurement. In this article, the former was applied. If there is a digital picture of a liquid drop or a gas bubble, contact angle can be measured directly by using the software of Photoshop or protractor through the shape photograph of the liquid drop or gas bubble. The distilled water and glycerine were used as titers. The average results are listed in Table 3, and typical photographs of liquid drops taken by digital camera are illustrated in Figures 3 and 4. Table 4 shows that the contact angle of

Table 2. The Values of TiO_2 Film Thickness of the Samples

Samples	A	B	C
Thickness of thin film, (m)	0	1.41×10^{-7}	1.587×10^{-6}

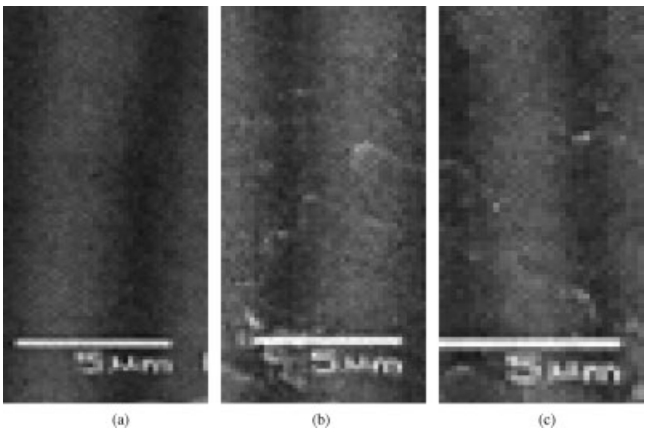

Figure 2. Surface topography of the samples by SEM.
(a) Sample A; (b) sample B; (c) sample C.

sample B is the largest one. Figures 3 and 4 indicate that the surface of the sample B is more difficult for wetting.

Calculation of Surface Free Energy. The magnitude of surface free energy is one of the important criterions to judge the difficult or ease degree of forming scale layer on the heated surface. When surface free energy of the material is high, the adsorption force of the surface to scale is great. The physical meaning of surface free energy is the necessary work done by overcoming the attractive force between two surfaces, and the value and dimension of surface free energy are the same as those of the surface tension. The surface tension is expressed by Young's equation:

$$\sigma_{sl} = \sigma_{sv} - \sigma_{lv}\cos\theta \tag{2}$$

Thus, surface free energy, E, is stated clearly by Dupre's equation:

$$E = \sigma_{lv} + \sigma_{sv} - \sigma_{sl} \tag{3}$$

The detail calculating method could be referred to the literature[25] and only the calculation results are shown in Table 4.

Table 4 shows that the surface free energy of uncoated surface (sample A) is maximum, and that of coated surface with film thickness of 1.41×10^{-7}m is minimum (sample B), and that of coated surface with film thickness of 1.587×10^{-6} m (sample C) is between above two samples. These facts mean that with the reducing of film thickness, surface free energy decreases, but there is a minimum of film thickness where its surface free energy is least.

Flow boiling heat transfer and antifouling experiments

Experimental Apparatus. Heat-transfer experimental setup is illustrated in Figure 5. The major sections are the double-pipe heat exchanger, separator, circulating tube, con-

Table 3. Contact Angles for Different Titers

Samples	A	B	C
Distilled water (°)	42	58	48
Glycerine (°)	79	87	80

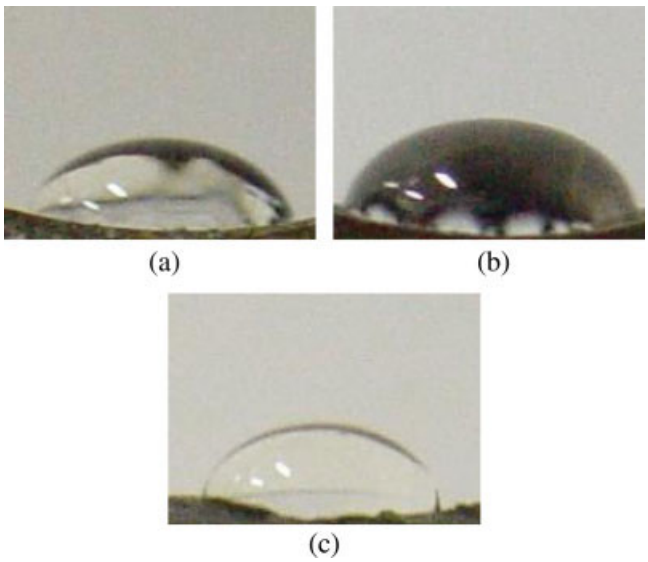

Figure 3. The liquid droplet on the different surface (glycerine as titer).

(a) Sample A; (b) sample B; (c) sample C. [Color figure can be viewed in the online issue, which is available at www.interscience.wiley.com.]

denser and electric boiler. The material of experimental apparatus is made of stainless steel in most runs, except specially mentioned. The double-pipe heat exchanger consisted of an inner tube and an outer tube. The inner tube is a seamless steel tube with inner diameter of 0.038 m and thickness of 0.002 m, and the inner diameter of outer tube is 0.144 m with thickness of 0.003 m. The heights of both inner and outer tubes are 1.0 m. The inner diameter of the separator is 0.25 m with height of 0.7 m. The inner diameter of circulating tube is 0.05 m with thickness of 0.002 m. The vapor condenser is a shell-

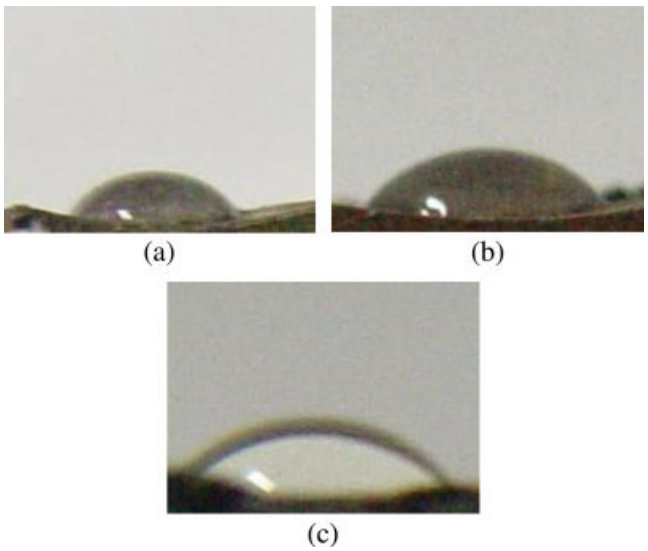

Figure 4. The liquid droplet on the different surface (distilled water as titer).

(a) Sample A; (b) sample B; (c) sample C. [Color figure can be viewed in the online issue, which is available at www.interscience.wiley.com.]

Table 4. The Values of Surface Free Energy of the Samples

Sample	A	B	C
$E \times 10^{-3}$ J m^{-2}	164.89	124.79	140.13

and-tube heat exchanger with the length of 1.0 m, outside diameter of 0.15 m and heat-transfer area of 0.5 m^2. The electrically heated boiler offer saturated steam for double-pipe heat exchanger. Five voltage regulators control the electric power and thus the vapor amount and pressure.

Experimental Fluid Medium and Operation Condition. Distilled water and saturated solution of calcium carbonate (SSCC) made at room temperature were used as the evaporated fluids. The reason of taking SSCC as heat transfer medium is that its solubility is relatively low and decreases along with the temperature increasing, as shown in Table 5.[26] Thus, the fouling is easy to form as the saturated solution temperature increasing, and the experimental time may be reduced. The main control parameter of the vapor–liquid boiling evaporation with natural circulating flow is saturated temperature of steam, T_s, ranging from 383.35 to 403.35 K or steam pressure, P_s.

Heat-Transfer Experimental Flowchart. As shown in Figure 5, when the fluid medium (distilled water or SSCC) in inner tube of double-pipe heat exchanger is heated by boiler steam to its boiling point, the boiling with external nature circulation flow caused by the density difference between the fluid in inner tube and that in circulating tube will take place. The fluid circulates along the inner tube, separator and circulating tube. When vapor–liquid mixture in inner tube gets into separator, the vapor phase will exhaust from upper exit, and then enters into vapor condenser to be cooled into liquid by cooling water. The condensate goes into condensate gauge bank. Flowing through the liquid pump, vapor condensate returns back to separator, where, it circulates again together with the liquid separated from the vapor–liquid mixture. The flow boiling evaporation is a continuous and steady process. After the saturated steam enters into the shell side of double-

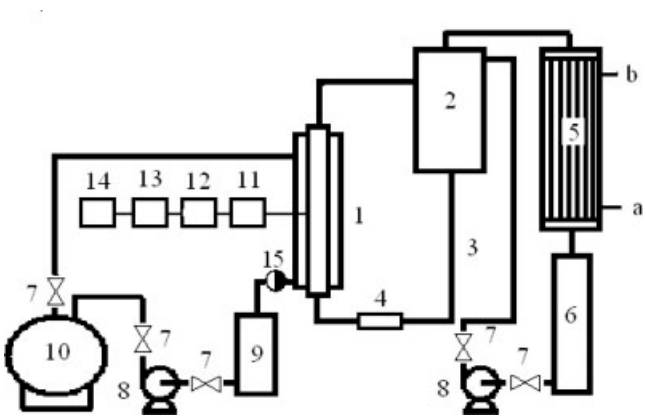

Figure 5. Heat transfer experimental apparatus system.

(1) Double-pipe heat exchanger; (2) separator; (3) circulating tube; (4) electromagnetic flowmeter; (5) vapor condenser; (6) vapor condensate gauge bank; (7) valve; (8) liquid pump; (9) boiler steam condensate gauge bank; (10) boiler; (11) Pt resistance sensor; (12) ample plate; (13) A/D plate; (14) PC; (15) steam trap. (a) inlet of cooling water; (b) outlet of cooling water.

Table 5. Solubility of the Calcium Carbonate

Temperature (°C)	0	10	20	30	40	50
Solubility $\times 10^{-5}$ kg $CaCO_3$/kg H_2O	8.1	7.0	6.5	5.2	4.4	3.8

pipe heat exchanger to heat the fluid in inner tube, it will be condensed into water. Then, passing the steam trap, it gets into steam condensate gauge bank. Afterwards, the steam condensate is pumped back into boiler.

Temperature Measurement. Temperature measured by thermocouple is affected by a series of environmental factors and a certain drift error may arise. Moreover, each thermocouple needs to be demarcated and calibrated. Therefore, thermocouple was not used here. Compared with thermocouple, platinum (Pt) resistance is an ideal transducer and Pt 100 type was selected to measure tube wall and fluid temperatures. Its precision scale is 0.0001 and heat response time is less than 0.05 s.

Five Pt resistance sensors were fixed on outside surface of inner tube with the same distance interval, 0.25 m to measure the wall temperature of inner tube. It is necessary to describe that Pt resistance sensors were inserted into the grooves on outside wall of inner tube closely, so as to assure the measurement accuracy. Three Pt resistance sensors were fixed at the inlet, middle location and outlet of inner tube to measure the fluid temperatures. Two Pt resistance sensors were fixed at the steam inlet and outlet of double-pipe heat exchanger to measure the steam temperatures in shell-side and that of steam condensate, respectively.

The pressure difference between the inlet and outlet of inner tube were measured with an electric capacity pressure transmitter (1151 DP type) with precision of 0.5. The external natural circulating flow rate and thus the circulating velocity of the fluid in inner tube was measured by an electromagnetic flow meter (LDT(50)122210 type) at an accuracy grade of 0.5 installed horizontally at the bottom of natural circulation system.[27]

Digitized signals of above parameters were recorded with a sample frequency of 10 Hz and the datum size of 100 points. The data were logged by the industrial computer 610 via a signal amplifier and an A/D converter with 12-bit resolution and accuracy better than 99.95%. The average values of above parameters were estimated and used for analysis.

The vapor and steam condensate rates were measured by volume method. The accuracy grades are 0.5 and 0.05 for graduated cylinder and chronograph, respectively.

Parameter Calculation. Heat-transfer flux, q was calculated with respect to inside surface area of heated tube by following two methods. One is based on the experimental data of vapor condensate and the other is on the data of boiler steam condensate. If the relative error of the two methods is less than 5%, the heat flux can be receptive. In this work, it is found that the average relative error is less than 4.6% and the heat flux calculated by the first method is taken as the heat flux for h_{fb} calculation.[28]

Flow boiling heat-transfer film coefficient, h_{fb} within heated tube was calculated by:

$$h_{fb} = \frac{q}{t_{iw} - t_f} \tag{4}$$

Pt resistance sensors were fixed on the outside surface of inner tube wall. Hence, the temperatures of inside surface of tube wall were calculated by the temperatures of outside surface of tube wall.

External natural circulating velocity of fluid in heated tube, u_c, was calculated on the data of circulating volume flow rate.

Fouling resistance was calculated by:

$$R_f = \frac{1}{h_{fb}} - \frac{1}{h_0} \tag{5}$$

It is noted that the coated surface was not exposed to the ultraviolet ray. Thus, the contact angle for given surface was constant during the experiments.

Results and discussion on heat transfer and antifouling experiments

Results and discussion on distilled water experiments

Figure 6 shows the relationship between heat transfer film coefficient of flow boiling and running time for different surface states at given saturated steam temperature. It can be found from Figure 6 that at given saturated steam temperature, boiling heat-transfer coefficient of inner tube undergoes no obvious variation with increase of running time, and increases with the increment of saturated steam temperature. Heat transfer coefficient on coated surface is higher than that on uncoated surface, and heat transfer coefficient on coated surface with film thickness of 1.41×10^{-7} m is higher than that with thickness of 1.587×10^{-6} m.

Figure 7 illuminates the relationship between average flow boiling heat transfer coefficient and thin layer thickness. It seems that the variation tendency is not monotonic and an optimum thickness of coated layer may exist. The possible mechanism for heat transfer enhancing effect of coated surfaces may be as followings. The micro-scale effect of nanometer thin layer may enhance the number of vaporization sites on flow boiling heat transfer.[29] However, if film thickness is too high, the heat resistance of thin film may reduce this enhancing effect.[19] Of course, more experimental investigations on heat-transfer surfaces coated with more different thicknesses are needed to support these conclusions other than only two thicknesses of the coating presented in this work.

In addition, Figures 8–10 also show the influences of heat flux, circulating velocity of fluid and pressure drop between inlet and outlet of the inner tube on the average boiling heat-transfer coefficients. Obviously, these variation rules agree well with the knowledge on flow boiling heat-transfer.

Results and discussion on experiments with SSCC

Surface free energy is a reflection of the unbalance force field on the heat transfer surface, and the unbalance force can adsorb the fouling deposits on the surface. Hence, if the adsorption force is weakened or surface free energy is low, the antifouling effect can be realized to some extent. Here, the investigations for the influences of surface state on fouling process are shown as follows. During the analysis, the heat resistance and heat transfer coefficient are used.

Before seamless steel tubes with coated surfaces are applied to carry out the antifouling experiment, an untreated brass tube with inner diameter of 0.038 m and thickness of

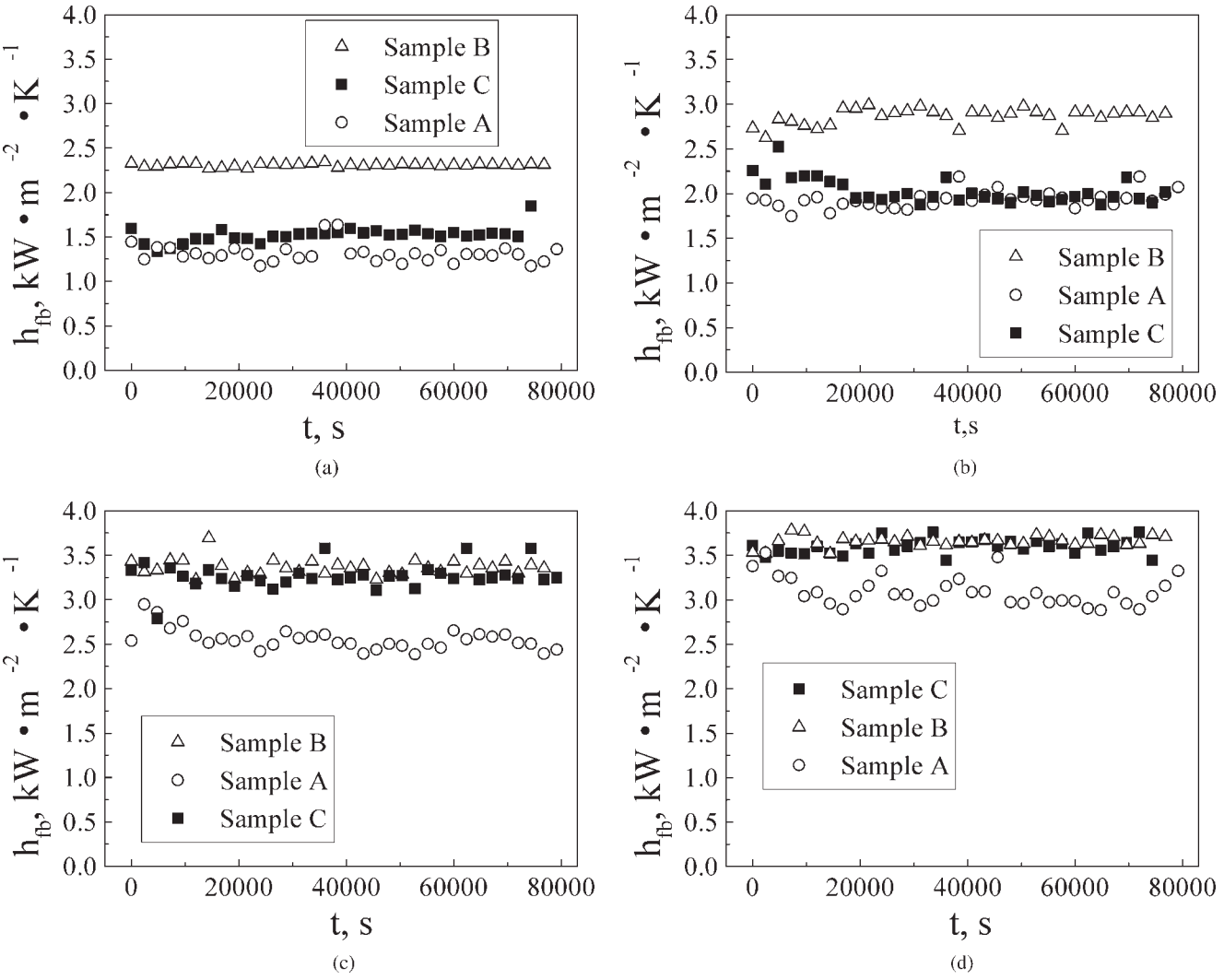

Figure 6. Heat-transfer coefficient of flow boiling vs. running time with different surfaces.

(a) T_s = 385.65 K; (b) T_s = 389.65 K; (c) T_s = 393.75 K; (d) T_s = 400.55 K.

0.002 m is first used to have a comparison with the results reported in open literature. Figure 11 shows the variations of heat transfer coefficient for flow boiling and fouling resistance with operating time for blank brass tube with SSCC.

From Figure 11 it can be said that the variation rules of the heat transfer coefficient of flow boiling and fouling resistance with operation time agree quite well with those reported in open literature.[30] For the evaporation of the SSCC, where the crystal fouling is dominant mechanism, boiling heat-transfer coefficient will come down along with running time prolonging after a slight increment at starting time. The reasons are as followings. At early stage of evaporating process, some crystal fouling can enhance heat transfer process since the crystallized particles layer often deposits on the heat-transfer surface discontinuously and augment nucleation boiling. However, when a continuous crystallized particle layer is formed on heat-transfer surface with the extension of operation time, inhibition action on boiling heat transfer will be dominant. In addition, the higher the heat flux, the higher the heat-transfer surface temperature. Thus, the more crystallized

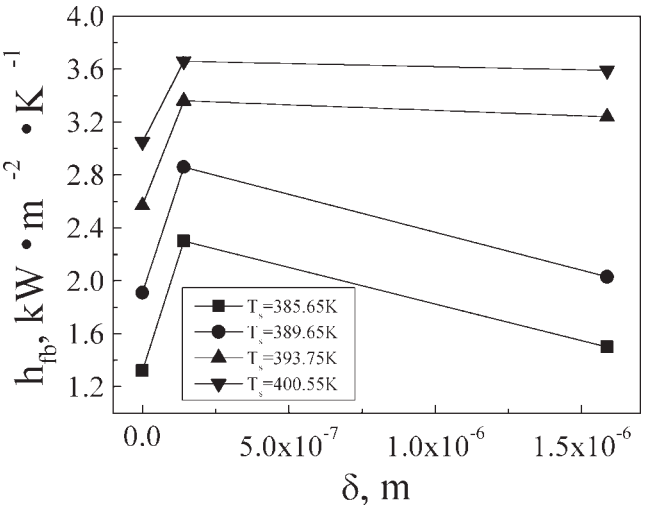

Figure 7. Average flow boiling heat-transfer coefficient and thin layer thickness.

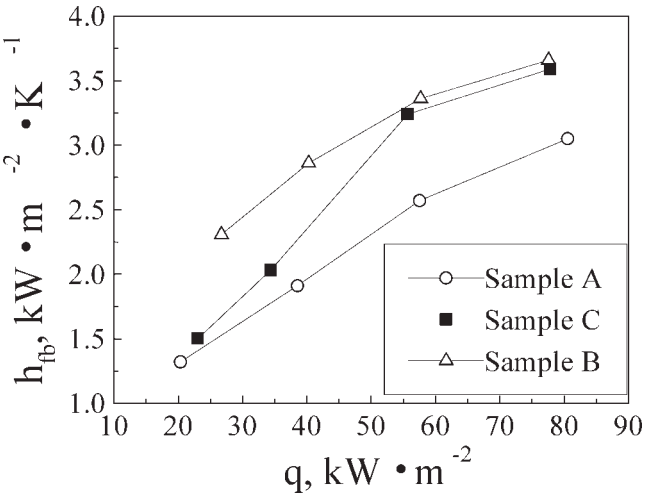

Figure 8. Average heat-transfer coefficient of flow boiling versus heat flux.

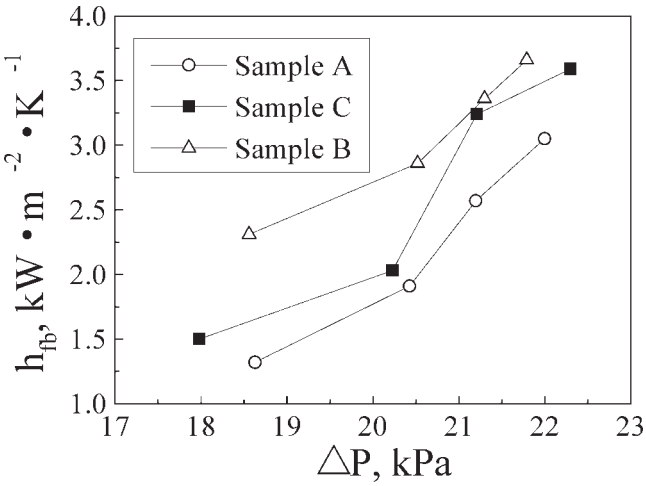

Figure 10. Average heat-transfer coefficient of flow boiling vs. pressure drop.

particles will deposit on heat-transfer surface, and the falling curve of heat-transfer coefficient will be steeper, as shown in Figure 11(a). Obviously, the variation tendency of fouling resistance along with operating time is near opposite to that of the heat-transfer coefficient, as shown in Figure 11(b). In Figure 11(b), one can also found that fouling resistance rises near linearly with the prolonging of operating time and heat flux has no obvious effect on fouling resistance. These rules agree well with the open literature.[30]

Figure 12 shows the heat-transfer coefficient, h_{fb} and fouling resistance, R_f with operating time for seamless steel tube in flow boiling system. If $CaCO_3$ crystal fouling is separated from supersaturated solution of calcium carbonate after a certain period of running time (called fouling induction period), it will precipitate over the heated surface and heat transfer coefficient of flow boiling will decrease, as shown in Figures 12 (a_1), (a_2), (a_3), and (a_4) for the samples A and C. On the other hand, the fouling resistance will increase continuously, as shown in Fig-

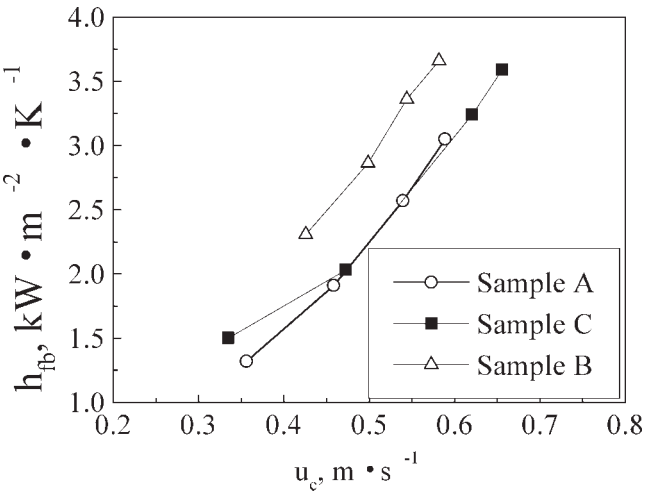

Figure 9. Average heat-transfer coefficient of flow boiling vs. circulating velocity of fluid.

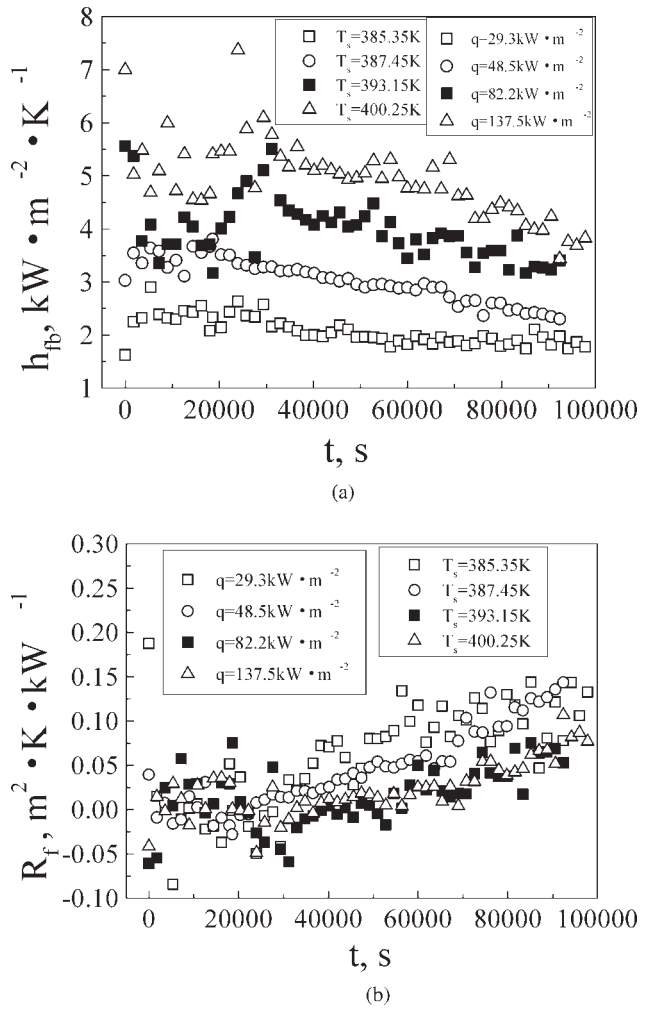

Figure 11. Heat-transfer coefficient of flow boiling or fouling resistance vs. operating time for untreated brass tube.

(a) Heat-transfer coefficient of flow boiling; (b) fouling resistance.

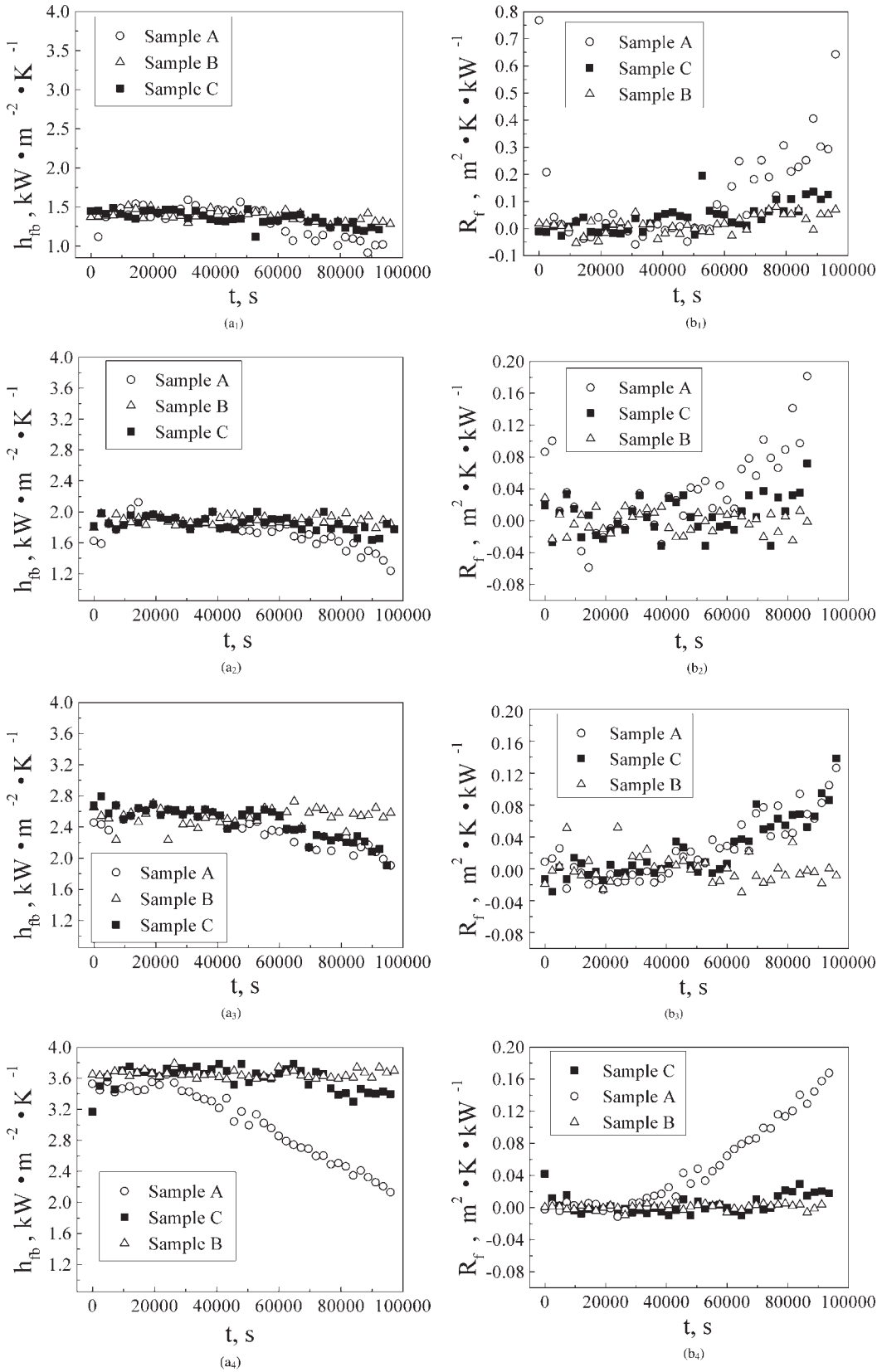

Figure 12. Heat-transfer coefficient of flow boiling or fouling resistance vs. operating time for coated surfaces.

(a_1), (a_2), (a_3), (a_4) Heat-transfer coefficient; (b_1), (b_2), (b_3), (b_4) fouling resistance. (a_1), (b_1) T_s = 387.55 K; (a_2), (b_2) T_s = 390.65 K; (a_3), (b_3) T_s = 393.95 K; (a_4), (b_4) T_s = 400.95 K.

ures 12 (b_1), (b_2), (b_3), and (b_4) for samples A and C. It seems from Figure 12 that the figure of fouling resistance makes the observation of fouling phenomenon clearer.

Compared with the uncoated surface of tube (sample A), the antifouling effect can clearly be observed from Figure 12 for coated surfaces (samples B and C) with TiO_2 thin layer. For coated tube with thickness of 1.41×10^{-7} m (sample B), no fouling is formed within the experimental time because no reduction of heat-transfer coefficient or no increasing of fouling resistance is observed from Figure 12, even though a slight fouling is found for coated tube with the thickness of 1.587×10^{-6} m (sample C), and a serious fouling is found for uncoated tube (sample A). This indicates that under the same experimental conditions, the thinner the nanometer material coated layer, the better the antifouling effect. Meanwhile, the higher the heat flux, the better the effect of preventing fouling because at higher heat flux, fouling is easier to form for the solution, as shown in Figures 12(a_4) and (b_4).

From Figure 12, the fouling induction period can also be obtained. For uncoated tube, the fouling induction period is about 48,000 s when saturated temperature is 387.55 K (Figure 12(b_1)), about 36,000 s when saturated temperatures are 390.65 and 393.95 K (Figures 12(b_2) and (b_3)), about 24,000 s when saturated temperature is 400.95 K (Figure 12(b_4)). For coated surfaces, the fouling induction period is enlarged and for coated surface with thickness of 1.41×10^{-7} m, no fouling is found in the present experimental conditions. The antifouling mechanism is largely contributed to the decrease of the surface free energy (see Table 4) because the surface free energy of the coated surface with thickness of 1.41×10^{-7} m is lowest. In addition, the micro-scale effect of nanometer thin layer may be another important cause.

The above results indicate that coated surfaces of TiO_2 thin film by using LPD method both have heat transfer enhancement and antifouling functions.

It is noted that the adhesion force of TiO_2 coating is high and no obvious peeling was found during the experiments.

Concluding Remarks

Coating some appropriate materials on heat-transfer surface with nanometer technology both to enhance flow boiling heat transfer and to inhibit fouling is the idea of this work. Nanometer TiO_2 was selected as the coated material, and the coated surface was prepared by LPD method and its thickness, contact angle and surface free energy, etc, were characterized.

Compared with the uncoated surface, heat-transfer enhancement was obtained with coated surfaces of TiO_2 film thickness of 1.41×10^{-7} and 1.587×10^{-6} m, and antifouling function of such coated layer tubes was also tested. The possible mechanism explanations were given on the characterization data of TiO_2 thin layer, such as the surface free energy, contact angle and thickness of thin layer etc.

The calculated and measured results of the surface free energy, contact angle and thickness of thin layer show that: $E_A > E_C > E_B$, $\theta_B > \theta_C > \theta_A$, and $\delta_C > \delta_B > \delta_A$. To enhance heat transfer and to prevent fouling, the best one is the coated layer tube with film thickness of 1.41×10^{-7} m, the better one is the coated tube with film thickness of 1.587×10^{-6} m, and the worst one is the uncoated tube. The coated tubes with δ of 1.41×10^{-7} and 1.587×10^{-6} m are better than that of uncoated tube on the performances of enhancing heat transfer and antifouling, and the thinner the film thickness, the better the above performances under present experimental conditions.

It seems from these results that heat-transfer enhancement is resulted from the hydrophobic surface and not from the hydrophilic or superhydrophilic surface, which is different from the literature,[18,19] in which superhydrophilic surface is ideal heat transfer surface.

The work is still in its very early stage and further work will be focused on the other thin film thickness, especially with nanometer scale; adhesion force of TiO_2 coating measurement; other coated materials, thin film preparation method; as well as the measurement methods with high accuracy.

Acknowledgments

The authors want to give their thanks to Nanjing Haitai Nanometer Technique Co, Ltd. and Prof. and Rui-tai Lin for their help in the preparation of thin film coated tube and the manuscript.

Notation

d = diameter of heated tube (m)
E = surface free energy (J m^{-2})
h = heat transfer coefficient (W m^{-2} K^{-1})
h_0 = heat transfer coefficient on clean heat-transfer surface (W m^{-2} K^{-1})
I = XRD integrated intensity, counts·(s^{-1})
I_∞ = XRD integrated intensity of bulk body, counts·(s^{-1})
Δp = pressure drop between inlet and outlet of heated tube, (Pa)
q = heat flux, (W m^{-2})
R_f = fouling resistance, (W^{-1} m^2 K^1)
T_s = saturated temperature, (K)
t = time, (s)
T_{iw} = inside surface temperature, (K)
T_f = fluid temperature, (K)
u = velocity, m s^{-1}

Greek letters

θ = diffraction angle, °; contact angle, °
δ = thickness of coated layer, (m)
σ = surface tension, (N m^{-1})
μ = Absorption coefficient, ($\mu = 5491.1$)

Subscripts

c = circulating
fb = flow boiling
i = inside
l = liquid
s = solid
v = gas
o = outside

Literature Cited

1. Hewitt GF, Shires GL, Bott TR. *Process Heat Transfer*. Boca Raton: CRC Press; 1994.
2. Bergles AE. Enhancement of pool boiling. *Int J Refrigeration*. 1997;20:545–551.
3. Khan N, Pinjala D, Toh KC. Pool boiling heat transfer enhancement by surface modification/micro-structures for electronics cooling: a review, Proceedings of 6th Electronics Packaging Technology Conference, Singapore, 2004. pp 273–280.

4. Webb RL, Donald Q. Kern lecture award paper: odyssey of the enhanced boiling surface, Transactions of the ASME. *J Heat Transfer*. 2004;126:1051–1059.
5. Bott TR. Aspects of crystallization fouling. *Exp Therm Fluid Sci*. 1997;14:356–360.
6. Yang SR, Xu EM, Sun LF. *The Fouling of Heat Exchanger and the Countermove*, 2nd Edition. Beijing: Science Press; 2004.
7. Mueller-Steinhagen H, Branch CA. Heat transfer and heat transfer fouling in Kraft black liquor evaporators. *Exp Therm Fluid Sci*. 1997;14:425–437.
8. Muller-Steinhagen H, Zhao Q. Investigation of low fouling surface alloys made by ion implantation technology. *Chem Eng Sci*. 1997; 52:3321–3332.
9. Ren XG, Liu JM, Liu CH, Zhao Q, Muller-Steinhagen H. Reduction of $CaSO_4$ scale formation during pool boiling by surface ion implantation. *J Chem Eng Chin Univ*. 2001;15:415–419.
10. Muller-Steinhagen H, Zhao Q, Helali-Zadeh A, Ren XG. Effect of surface properties on CaSO4 scale formation during convective heat-transfer and subcooled flow boiling. *Can J Chem Eng*. 2000;78: 12–20.
11. Santos O, Nylander T, Rosmaninho R, Rizzo G, Yiantsios S, Andritsos N, Karabelas A, Muller-Steinhagen H, Melo L, Boulange-Petermann L, Gabet C, Braem A, Tragardh C, Paulsson M. Modifed stainless steel surfaces targeted to reduce fouling–surface characterization. *J Food Eng*. 2004;64:63–79.
12. Rosmaninho R, Melo LF. Calcium phosphate deposition from simulated milk ultrafiltrate on different stainless steel-based surfaces. *Int Dairy J*. 2006;16:81–87.
13. Vassallo P, Kumar R, Damico S. Pool boiling heat-transfer experiments in silica-water nano-fluids. *Int J Heat Mass Transfer*. 2004; 47:407–413.
14. Vadasz JV, Govender S, Vadasz P. Heat transfer enhancement in nano-fluids suspensions: possible mechanisms and explanations. *Int J Heat Mass Transfer*. 2005;48:2673–2681.
15. Takata Y, Tanaka K, Kaijima K, Ito T, Watanabe T, Shimohigoshi M. Enhancement of boiling and evaporation heat transfer by superhydrophilic photocatalyst. Proceedings of the 6th UK National Conference on Heat Transfer, 1999. pp 323–238.
16. Takata Y, Hidaka S, Cao JM, Tanaka K, Masuda M, Ito T, Watanabe T, Shimohigoshi M. Boiling and evaporation from a superhydrophilic surface. *Therm Sci Eng*. 2000;8:33–41.
17. Hidaka S, Yamasita A, Yamamoto H, Takata Y, Ito T. Increase in hydrophilicity by plasma irradiation and evaporation of water drop. *Therm Sci Eng*. 2002;10:31–32.
18. Takata Y, Hidaka S, Masuda M, Ito T. Pool boiling on a superhydrophilic surface. *Int J Energy Res*. 2003;27:111–119.
19. Takata Y, Hidaka S, Cao JM, Nakamura T, Yamamoto H, Masuda M, Ito T. Effect of surface wettability on boiling and evaporation. *Energy*. 2005;30:209–220.
20. Niesen TP, De Guire MR. Review: deposition of ceramic thin films at low temperatures from aqueous solutions. *Solid State Ionics*. 2002;151:61–68.
21. Gao YF, Koumoto K. Bioinspired ceramic thin film processing: present status and future perspectives. *Cryst Growth Des*. 2005;5:1983–2017.
22. Dax M. X-ray film thickness measurement. *Semicond Int*. 1996,19:6–9.
23. Yashar PC, Sproul WD. Nanometer scale multilayered hard coatings. *Vacuum*. 1999;55:179–190.
24. Lhotka J, Kuzel R, Cappuccio G, Valvoda V. Thickness determination of thin polycrystalline film by grazing incidence X-ray diffraction. *Surf Coat Technol*. 2001;148:96–101.
25. Michalski MC, Hardy J, Saramago BJ. On the surface energy of PVC/EVA polymer blends comparison of fifferent calculation methods. *J Colloid Interface Sci*. 1998;208:319–328.
26. Liu GQ, Ma LX, Liu JL. *The Handbook of Chemical Industry and Chemistry Property Data*. Beijing: Chemical Industry Press. 2002.
27. Liu MY, Qiang AH, Sun BF. Chaotic characteristics in an evaporator with a vapor-liquid-solid boiling flow. *Chem Eng Process*. 2006; 45:73–78.
28. Liu MY, Nie WD, Yang Y, Ling NS, Li XL. Concentration of Gengnian'an Extract with a Vapor-Liquid-Solid Evaporator. *AIChE J* 2005;51:759–765.
29. Liu J. *The Heat Transfer Within Micro-Nano Scale*. Beijing: Science Press; 2002.
30. Najibi SH, Muller-Steinhagen H, Jamialahmadi M. Calcium sulphate scale formation during subcooled flow boiling. *Chem Eng Sci*. 1997;52:1265–1284.

Manuscript received July 21, 2006, and revision received Jan. 4, 2007.